




Activation of astroglial CB₁R mediates cerebral ischemic tolerance induced by electroacupuncture

Cen Yang^{1,2,*}, Jingjing Liu^{1,3,4,*}, Jingyi Wang^{1,3,4}, Anqi Yin¹, Zhenhua Jiang¹, Shuwei Ye³, Xue Liu^{3,4}, Xia Zhang^{1,5}, Feng Wang^{1,3}  and Lize Xiong^{1,6}

Abstract

There are no effective treatments for stroke. The activation of endogenous protective mechanisms is a promising therapeutic approach, which evokes the intrinsic ability of the brain to protect itself. Accumulated evidence strongly suggests that electroacupuncture (EA) pretreatment induces rapid tolerance to cerebral ischemia. With regard to mechanisms underlying ischemic tolerance induced by EA, many molecules and signaling pathways are involved, such as the endocannabinoid system, although the exact mechanisms have not been fully elucidated. In the current study, we employed mutant mice, neuropharmacology, microdialysis, and virus transfection techniques in a middle cerebral artery occlusion (MCAO) model to explore the cell-specific and brain region-specific mechanisms of EA-induced neuroprotection. EA pretreatment resulted in increased ambient endocannabinoid (eCB) levels and subsequent activation of ischemic penumbral astroglial cannabinoid type I receptors (CB₁R) which led to moderate upregulation of extracellular glutamate that protected neurons from cerebral ischemic injury. These findings provide a novel cellular mechanism of EA and a potential therapeutic target for ischemic stroke.

Keywords

Astrocyte, CB₁R, electroacupuncture, pretreatment, stroke

Received 5 November 2020; Revised 15 January 2021; Accepted 18 January 2021

Introduction

Ischemic stroke is the second most common cause of death worldwide and the leading cause of disability in both the United States and China.^{1–4} The most-prescribed treatments of ischemic stroke, recommended by current guidelines, are the intravenous thrombolysis of tissue plasminogen activator (tPA) and mechanical thrombectomy.⁵ Administration of alteplase between

4.5 and 9.0 hours after stroke onset, or at the time the patient awakes with stroke symptoms, results in a higher percentage of patients with no, or minor, neurologic deficits than after administration of placebo.⁶ However, the successful delivery of mechanical thrombectomy requires specialized stroke centers and trained

¹Department of Anesthesiology and Perioperative Medicine, Xijing Hospital, Fourth Military Medical University, Xian, Shaanxi Province, China

²Shenzhen University General Hospital, Shenzhen University, Shenzhen, Guangdong Province, China

³The Brain Cognition and Brain Disease Institute, Shenzhen Institutes of Advanced Technology, Chinese Academy of Science; Shenzhen-Hong Kong Institute of Brain Science-Shenzhen Fundamental Research Institutions, Shenzhen, China

⁴University of the Chinese Academy of Sciences, Beijing, China

⁵University of Ottawa Institute of Mental Health Research at the Royal, Department of Psychiatry, and Department of Cellular & Molecular Medicine, Ottawa, Canada

⁶Translational Research Institute of Brain and Brain-Like Intelligence, Shanghai Fourth People's Hospital Affiliated to Tongji University School of Medicine, Shanghai, China

*These authors contributed equally to this work.

Corresponding authors:

Lize Xiong, Department of Anesthesiology and Perioperative Medicine, Xijing Hospital, Fourth Military Medical University, 127 Changle West Road, Xi'an, Shaanxi 710032, China.

Email: mzkxlz@126.com

Feng Wang, The Brain Cognition and Brain Disease Institute, Shenzhen Institute of Advanced Technology, Chinese Academy of Sciences, Shenzhen 518055, China.

Email: feng.wang@siat.ac.cn

professional staff.⁷ Thus, the need for effective stroke prevention and treatment is an urgent medical problem.

It has been suggested that preconditioning methods, such as HBO preconditioning,⁸ lipopolysaccharide,⁹ brief ischemia¹⁰ and peroxisome proliferator-activated receptor- α activation,¹¹ evoke endogenous protective mechanisms as a potential treatment for stroke.¹² Electroacupuncture (EA), based on traditional acupuncture combined with modern electrotherapy, is a relatively safe, cheap, and straight forward therapy and widely accepted by patients. Animal studies have shown that EA pretreatment may produce neuroprotective effects.^{13,14} Our previous work has demonstrated that EA pretreatment exerts a neuroprotective effect by reducing the ischemic infarct volume, which is accompanied by an increase in neurological scores in rats.¹⁵ Moreover, EA pretreatment elicited the eCBs, which subsequently activated the cannabinoid 1 receptor (CB₁R) to produce cerebral ischemia protection.^{16–18} These studies suggest that EA pretreatment may be a promising clinical application for cerebral ischemia protection and that the eCB system may regulate ischemic tolerance induced by EA. However, the specific neural mechanisms underlying regulation by the eCB system of ischemic tolerance induced by EA pretreatment, such as the specific neurological cells that release eCBs and express the CB₁R that modulate the neuroprotective effect, have not yet been determined.

Endocannabinoids, such as 2-arachidonoylglycerol (2-AG) and anandamide, influence a broad range of functions, including learning, memory and neuroprotection.^{19,20} For example, diacylglycerol lipase α (DAGL α) is responsible for the biosynthesis of 2-AG,²¹ the most abundant eCB in the brain. Postsynaptic neuron-released 2-AG acts retrogradely on presynaptic CB₁R, which is the most abundant G protein-coupled receptor in the central nervous system,^{22,23} to produce its specific functions. Classically, CB₁R was found to be mainly present in presynaptic terminals,²⁴ mostly in GABAergic interneurons but it is also found at low levels on glutamatergic neurons and astrocytes.²⁵

Astroglial CB₁R play an important role in maintaining many brain functions, such as the memory formation of cannabis addiction,²⁶ the cannabis-induced impairment of spatial memory²⁷ and the rapid anti-anxiety of fatty acid amide hydrolase (FAAH) inhibition.²⁸ Our recent work demonstrated that JZL195 induced long-term depression (LTD) by astroglial CB₁R *in vivo* and produced a neuroprotective effect against ischemic insult.²⁹ This suggests a crucial role of astroglial CB₁R in ischemic tolerance in the brain. However, whether astroglial CB₁R are involved in EA has not yet been shown.

Excessive glutamate release plays an important role in the pathophysiology of brain ischemia.³⁰ Excitatory amino acid transporter 2 (EAAT2) is primarily found on perisynaptic processes of astrocytes³¹ and is responsible for approximately 90% of the content of excitatory neurotransmitter glutamate in the synaptic gap.³² Knockdown of EAAT2 exacerbates the damage of transient middle cerebral artery occlusion-induced ischemic stroke.³³ In contrast, overexpression of EAAT2 enhances neuroprotection following moderate oxygen glucose deprivation *in vitro*³⁴ and reduces infarct volume in a middle cerebral artery occlusion (MCAO) model *in vivo*.³⁵ Kano et al. demonstrated that activation of astroglial CB₁R increased the concentration of extracellular glutamate.³⁶ Therefore, we hypothesize that an increase of ambient eCB induced by EA pretreatment, as well as the subsequent activation of ischemic penumbral astroglial CB₁R, up-regulates EAAT2 and then leads to the moderate upregulation of extracellular glutamate, ultimately producing neuronal protection against lethal ischemic insults, which will benefit those with a high risk of ischemic stroke in the perioperative period.

Materials and methods

Animals

Male C57BL/6J mice at 6–8 weeks old and weighing 22–25 g were used (Beijing Vital River Laboratory Animal Technology Co., Ltd., Beijing, China). They were housed under a 12:12 light-dark cycle with room temperature maintained at 22 ± 1°C and allowed free access to food and water. The experimental protocol used in this study was approved by the Fourth Military Medical University Animal Ethics Committee and was conducted in accordance with the Guidelines for Animal Experimentation of the Fourth Military Medical University (Xi'an, China), and reported according to the ARRIVE (Animal Research: Reporting In Vivo Experiments) guidelines.³⁷ All efforts were made to minimize both suffering and the number of mice used.

Generation of mutant mice

CB₁R-floxed,^{29,38} vGLUT1-iCreERT2³⁸ and GAD2-iCreERT2³⁸ mutant mice were generated by Beijing Biocytogen Co., Ltd., (Beijing, China), as described previously. GFAP-CreERT2^{29,39} mutant mice were purchased from Model Animal Research Center of Nanjing University.

The CB₁R-floxed mice were crossed with vGLUT1-iCreERT2, GAD2-iCreERT2 or GFAP-CreERT2 mutant mice to generate vGLUT1-CB₁R-KO, GAD2-

CB₁R-KO and *GFAP-CB₁R*-KO mouse lines using protocols described previously.^{29,38,39} These seven mouse lines and all *iCreERT2* mice received eight daily injections of tamoxifen (Sigma, Missouri, USA, 10 mg/ml, 0.1 ml/d, dissolved in 90% sunflower oil, i.p.) two weeks before experiments.

Electroacupuncture

Mice were anesthetized using 1.0 MAC (1.4%) isoflurane at 1.0 L/min with 100% oxygen and stimulated with EA (G6805-2 EA Instrument, Model No. 227033, Qingdao Xinheng Ltd., Qingdao, Shandong, China) at the Baihui acupoint (GV 20), which is located at the intersection of the sagittal midline and the line linking the right side of the mouse ears. An intensity of 1 mA and frequency of 2/15 Hz were selected for the EA administration as described in our previous work.¹⁵ A fine needle (0.5 mm diameter) placed at GV 20 was connected to one EA stimulator electrode and to the other electrode on the right ear. Tremor of the ears during administration was regarded as effective EA stimulation. Mice core temperatures of the were maintained at $37.0 \pm 0.5^\circ\text{C}$ by surface heating or cooling during anesthesia and EA.

Induction of transient focal cerebral ischemia

Under isoflurane anesthesia (3% for induction and 1.4% for maintenance; maintenance under 100% O₂), the right-hand common carotid arteries were exposed, isolated from the adjacent nerve and tissue, and then occluded for 60 minutes using microclips (0.23 mm \times 0.126 mm/3 cm, RWD Inc., Shenzhen, China) to induce transient focal cerebral ischemia, which was followed by reperfusion. To prevent the occurrence of hypothermia during surgery, rectal temperature was maintained at $37 \pm 0.5^\circ\text{C}$ using a heating pad. Seventy-two hours following reperfusion, all experimental animals were sacrificed for further experimental procedures.

Neurological evaluation and 2, 3, 5-Triphenyltetrazolium chloride staining

Seventy-two hours after reperfusion, a neurological assessment of the mice in different groups was performed by an investigator blind to experimental conditions, using the 18-point scoring system reported by Gracia et al.⁴⁰ The system consisted of spontaneous activity, side stroking, vibrissa touch, limb symmetry, and climbing and forelimb walking assessments. After neurological evaluation, mice were decapitated, and brains were rapidly removed and mildly frozen to keep morphology intact during slicing. Infarct volume was measured as described previously.^{15,41} In brief, the

brain was rapidly dissected and sectioned into six coronal blocks in a brain matrix with an approximate thickness of 1 mm and stained with 2% (w/v) 2, 3, 5-triphenyltetrazolium chloride (TTC) (Sigma, Missouri, USA) for 30 minutes at 37°C followed by overnight immersion in 4% (w/v) paraformaldehyde. The infarct tissue area remained unstained (white), whereas normal tissue was stained red. Infarct areas on each slice were demarcated and analyzed using image pixels and Adobe Photoshop CC (2014; Adobe, San Jose, CA, USA). The total infarct volumes were calculated according to the following formula: ((total contralateral hemispheric volume) - (total ipsilateral hemispheric stained volume))/(total contralateral hemispheric volume) \times 100%.

Mouse surgery

Male C57BL/6 mice or mutant mice (weighing 22–25 g) underwent surgeries for implantation of a guide cannula for a microinjection needle and microdialysis needle. During pentobarbital anesthesia (50 mg/kg, intraperitoneal), a guide cannula (O.D. $0.48 \times$ I.D. 0.34, RWD Inc., Shenzhen, China) for the microinjection needle (O.D. $0.30 \times$ I.D. 0.14, RWD Inc., Shenzhen, China) was directed stereotaxically at the lateral ventricles. A guide cannula (Eicom Corporation, Kyoto, Japan) for microdialysis (membrane length, 1 mm; OD, 0.22 mm; cut off size, 20 kDa; Eicom Corporation, Kyoto, Japan) was directed stereotaxically at the ischemic penumbra. The tip of the microinjection and microdialysis needle was 1 mm longer than the tip of the guide cannula. The coordinates of the probe tip according to the Paxinos and Watson mouse brain atlas were AP -0.4 mm from bregma, ML $+1.0$ mm, DV -2.5 mm (lateral ventricles) and AP $+0.5$ mm, ML -1.2 mm, DV -0.8 mm for the ischemia penumbra. Mice were permitted to recover for at least seven days before any treatment.

Microdialysis

Animals were single-housed following implantation of the microdialysis probe for the remainder of the experiment. During dialysis, aCSF solution (145 mM NaCl, 2.8 mM KCl, 1.2 mM MgCl₂, 1.26 mM CaCl₂, and 5.4 mM d-glucose (pH 7.4)) was pumped through the microdialysis probe at 1 $\mu\text{L}/\text{min}$. Dialysis samples were collected every 30 minutes and stored on dry ice during the experiment, and then samples were stored at -80°C until analyzed for glutamate content using liquid chromatography coupled with mass spectrometry. After a 2-hour balance period, seven samples were collected per mouse. The first sample collected was used as a baseline. Then, one sample was collected when mice

were randomly assigned to an electroacupuncture (EA) group or sham electroacupuncture (sham) group during isoflurane anesthesia for 30 minutes. The subsequent five samples were gathered after the EA/sham treatment when mice were freely moving. Samples were stored at -80°C until detection analysis.

High performance liquid chromatography analysis of glutamate

The concentrations of glutamate were analyzed using High Performance Liquid Chromatography (HPLC) (Agilent 1100, Agilent, California, USA) with fluorescence detection. The microdialysis samples were pre-column derivatized with 2,4-dinitrofluorobenzene for 30 minutes at 60°C , and then 50 mM potassium dihydrogen phosphate was added to each microdialysis sample mixture to stop the reaction. The microdialysis sample mixtures were then filtered using a $0.22\text{-}\mu\text{m}$ filter (Agilent C18; $4.6 \times 250\text{ mm}$, $5\text{ }\mu\text{m}$). The mobile phase consisted of 99% methanol and 0.1 M sodium acetate buffer (pH 8.0) at a flow rate of 1.0 mL/min, and the column temperature was maintained at 35°C . A UV detector was operated at an excitation wavelength of 250 nm and an emission wavelength of 410 nm to analyze neurotransmitter concentrations in the microdialysis samples. Concentrations were calculated using Agilent Chemstation (B.04.02 SP1) based on standard samples (Sigma-Aldrich, Missouri, USA).

DREADD strategy

We used the Designer Receptors Exclusively Activated by Designed Drugs (DREADD) technique to modulate the activity of ischemic penumbra astrocytes. All DREADD viruses, including AAV2/9-EF1 α -DIO-mCherry-WPRE-pA (AAV-mCherry), AAV2/9-EF1 α -DIO-hM3Dq-mCherry-WPRE-pA (AAV-hM3Dq-mCherry) and AAV2/9-EF1 α -DIO-hM4Di-mCherry-WPRE-pA (AAV-hM4Di-mCherry) were purchased from the Brain VTA company (WuHan, China). Aliquots of virus vectors were stored at -80°C before use in intra-ischemia penumbra micro-injections. On the day of surgery, stocks were thawed, cell debris was pelleted by centrifugation at high speed (4000 rpm for 1 minute) in a bench-top centrifuge, and the supernatant was carefully collected for injection. Under isoflurane anesthesia, AAV-mCherry or AAV-hM3Dq-mCherry/AAV-hM4Di-mCherry (5×10^{12} genome copies per mL) was injected into the right primary motor cortex (AP +0.5 mm, ML -1.2 mm , DV -0.8 mm) of GFAP-Cre mice using a Hamilton syringe (7001KH) at a rate of $0.1\text{ }\mu\text{L}/\text{min}$ for 3 minutes. Four weeks later, all mice were given clozapine (CNO; Caymen Chemical, Ann Arbor, MI, USA; 3 mg/kg, i.

p. dissolved in dimethylsulfoxide (DMSO)) before EA treatment, and the AAV-hM4Di-mCherry and AAV-mCherry groups received EA for 30 minutes. Two hours after EA administration, we induced MCAO in these three mice groups. Seventy-two hours after reperfusion, neurological testing was carried out, followed by brain extraction for TTC staining.

Specific CB₁R deletion

The CB₁R-floxed mice were used for virus-mediated conditional deletion of astroglial CB₁R in the ischemic penumbra by injection of AAV2/9-GFAP-Cre-WPRE-pA (GFAP-Cre) or AAV2/9-GFAP-EYFP-WPRE-pA (GFAP-EYFP) into the right primary motor cortex (AP +0.5 mm, ML -1.2 mm , DV -0.8 mm). Viruses were purchased from the Brain VTA company (WuHan, China). Four weeks later, all mice were administered EA for 30 minutes. Two hours after EA, MCAO was induced. Mice were scored in neurological tests 72 hours after reperfusion, followed by brain extraction for TTC staining.

Procedures and drugs

To investigate the effect of EA treatment after the onset of ischemic stroke, 30 minutes of EA treatment was administered 24 hours after middle cerebral artery occlusion (MCAO) by an intraluminal filament technique as described previously.⁴² Reperfusion was accomplished by withdrawing the suture 60 minutes after ischemia. Infarct volume and neurological scores were evaluated 72 hours after reperfusion.

To investigate the role of CB₁R in the EA treatment after ischemic stroke, 30 minutes of EA stimuli was performed 24 hours after MCAO, whilst cannabinoid receptor antagonist AM281 (Tocris Bioscience, Ellisville, Missouri, USA; 3 mg/kg, i.p, dissolved in $1 \times \text{DMSO}:1 \times \text{Tween } 80:18 \times \text{physiological saline}$) or vehicle was injected 15 minutes before EA.^{38,42} Reperfusion was accomplished by withdrawing the suture 60 minutes after ischemia. Infarct volume and neurological scores were evaluated 72 hours after reperfusion.

To explore the early effect of EA pretreatment, EA stimuli was administered daily for 30 minutes for 5 consecutive days. MCAO surgery was performed 28 days after the 5th consecutive EA treatment. Reperfusion was accomplished by withdrawing the suture 60 minutes after ischemia. Infarct volume and neurological scores were calculated 72 hours following reperfusion.

To identify whether EA pretreatment triggered an increase in the synaptic cleft 2-AG-induced neuroprotective effect, pharmacological interventions were

conducted at different times prior to EA, according to specific protocols. This was followed 2 hours later by reperfusion and then another 72 hours later by neurological evaluation. The 2-AG inhibitor RHC80267 (Tocris Bioscience, Ellisville, Missouri, USA; 0.1 µg/5 µL, i.c.v. dissolved in 1 × DMSO: 1 × Tween 80:18 × physiological saline) or vehicle⁴³ was microinjected into the lateral ventricles 1 hour before EA administration. The monoacylglycerol lipase inhibitor JZL184 (Tocris Bioscience, Ellisville, Missouri, USA; 20 mg/kg, i.p., dissolved in 1 × DMSO:1 × Tween 80:8 × physiological saline) or vehicle²⁹ was administered by intraperitoneal injection 12 hours before MCAO induction. The FAAH inhibitor PF3845 (Tocris Bioscience, Ellisville, Missouri, USA; 10 mg/kg, i.p., dissolved in 1 × DMSO:1 × Tween 80:18 × physiological saline)⁴⁴ was administered 2 hours before MCAO induction.

To investigate the role of CB₁R in the neuroprotective effect of EA pretreatment, CB₁R antagonists were administered before EA. Either AM281 (Tocris Bioscience, Ellisville, Missouri, USA; 3 mg/kg, i.p. dissolved in 1 × DMSO:1 × Tween 80:18 × physiological saline) or vehicle, and either NESS0327 (Tocris Bioscience, Ellisville, Missouri, USA; 0.3 mg/kg, dissolved in 1 × DMSO:1 × Tween 80:18 × physiological saline) or vehicle³⁸ was administered by i.p. injection 15 minutes before EA.

To identify the function of EAAT2 in the neuroprotection of the EA pretreatment, pharmacological interventions were conducted to stimulate or inhibit the activity of EAAT2. Either LDN 212,320 (Tocris Bioscience, Ellisville, Missouri, USA; 40 mg/kg i.p., dissolved in 1 × DMSO:1 × Tween 80:18 × physiological saline) or vehicle was administered by i.p. injection 15 minutes before EA, and either Ceftriaxone (Roche, Basel, Switzerland; 200 mg/kg once per day for 5 consecutive days, i.p., dissolved in physiological saline) or saline administered by i.p. injection once a day for five consecutive days before MCAO induction. In addition, dihydrokainic acid (DHKA; Tocris Bioscience, Ellisville, Missouri, USA; 10 mg/kg, i.p., dissolved in 1 × DMSO:1 × Tween 80:8 × physiological saline) or vehicle was administered by i.p. injection 30 minutes before EA.

To clarify the relationship between EAAT2 and astroglial CB₁R in the neuroprotective effect of EA pretreatment, the EAAT2 translational activator, LDN 212,320 (Tocris Bioscience, Ellisville, Missouri, USA; 40 mg/kg i.p. dissolved in 1 × DMSO: 1 × Tween 80:18 × physiological saline) or vehicle administered by i.p. injection 15 minutes before EA in GFAP-CB₁R-KO mice. Two hours after 30 minutes of EA administration, MCAO was induced. Reperfusion was accomplished by withdrawing the suture

60 minutes after ischemia. Infarct volume and neurological scores were evaluated 72 hours after reperfusion.

Neurological deficit evaluation and cresyl violet staining

Cresyl violet staining was performed to observe morphological changes in cells within the ischemic penumbra following MCAO. Animals were sacrificed 28 days post-stroke. Mice in each group were anesthetized and transcardially perfused with physiologic saline followed by 4% paraformaldehyde (PFA). Brains were subsequently removed, fixed in 4% formaldehyde solution at 4°C post-fixation, then immersed successively in 20% and 30% sucrose until they sank. Brain samples were sectioned with a Leica CM1900 cryostat (Leica Microsystems GmbH, Wetzlar, Germany) into 12-µm coronal sections. For each brain, six sequential sections were taken at 100-µm intervals and processed for cresyl violet staining. Frozen sections were stained with 0.1% cresyl violet (Sigma-Aldrich Corporation, Saint Louis, Mo., USA) solution for 10 minutes at room temperature, rinsed with PBS, dehydrated in a graded series of alcohol, cleared in xylene, and then mounted with neutral gum. The sections were observed using light microscopy. The total number of damaged neurons in the ischemic penumbra was counted in five different fields of view for each section by an observer, blind to the treatment group, using light microscopy at ×400 magnification (BX51; Olympus, Tokyo, Japan). Infarct volume was measured using ImageJ analysis software (version 1.46r; National Institutes of Health, Bethesda, MD, USA).

At 7, 14, and 28 days following reperfusion, a neurological deficit assessment of mice in the different groups was performed by two investigators blind to the group assignment, using the 28-point scoring system reported by Clark.⁴⁵ Two investigators blind to the group assignment independently identified and scored individual animals, which were then averaged.

Statistics

All results except the neurological scores are expressed as the mean ± SD. Statistical analysis of the data was performed using a student's *t*-test or one-way ANOVA, followed by Bonferroni or LSD post-hoc tests. Neurological scores are expressed as the median (range) and analyzed with the Kruskal–Wallis followed by the Mann–Whitney U tests. Group differences in baseline dialysate glutamate concentrations were evaluated using a one-way ANOVA with EA treatment as the between-subjects factor. Dialysate glutamate levels

for each treatment group are expressed as a percentage of mean baseline dialysate concentration (set at 100%) and repeated-measures ANOVA was used to test group differences in dialysate glutamate levels following EA treatment. In the case of significant overall effects, Bonferroni multiple comparison correction was applied for post-hoc comparisons. The level of probability for a statistically significant effects was set at 0.05. Anderson-Darling, D'Agostino-Pearson omnibus normality, Shapiro-Wilk normality, and Kolmogorov-Smirnov normality tests were carried out to conform with journal guidelines, when applicable. All graphs were produced using GraphPad Prism 6 for Mac (GraphPad Software, San Diego).

Results

EA pretreatment-induced eCB activates CB₁R and produces cerebral ischemic tolerance

Neuropharmacological agents were used to investigate the role of neuroprotection following EA induced by 2-AG, one of the major endogenous agonists of eCB which acts predominantly on canonical presynaptic CB₁R in a retrograde manner to inhibit neurotransmitter release. Following TTC staining and a

neurological score evaluation, we observed that i.c.p injection of the 2-AG synthetase inhibitor RHC80267 led to markedly decreased 2-AG brain levels, similar to inhibition or deletion of CB₁R. This resulted in an increase in infarct volume at 72 hours after EA administration and ischemic reperfusion (Figure 1(a) and (b)), as well as a decrease in neurological scores (Figure 1(c)). This suggests that EA-induced neuroprotection is 2-AG and CB₁R dependent. This was further supported by our finding that systemic administration of the 2-AG hydrolase inhibitor JZL184, which increased 2-AG levels in the brain and activated presynaptic CB₁R, led to lower infarct volume (Figure 1(d) and (e)) and improved neurological scores (Figure 1(f)) compared to vehicle, which mimicked the neuroprotection of EA.

There was no difference in infarct volume between the EA treatment and sham EA groups after MCAO (sFigure 1(a)), whereas neurological scores were higher in the EA treatment group (sFigure 1b). No significant differences in infarct volume (sFigure 2(a)) or neurological scores (sFigure 2(b)) were observed between the vehicle and the AM281-treated group, suggesting that EA treatment after MCAO does not lead to neuroprotection, and that CB₁R were not involved in the process.

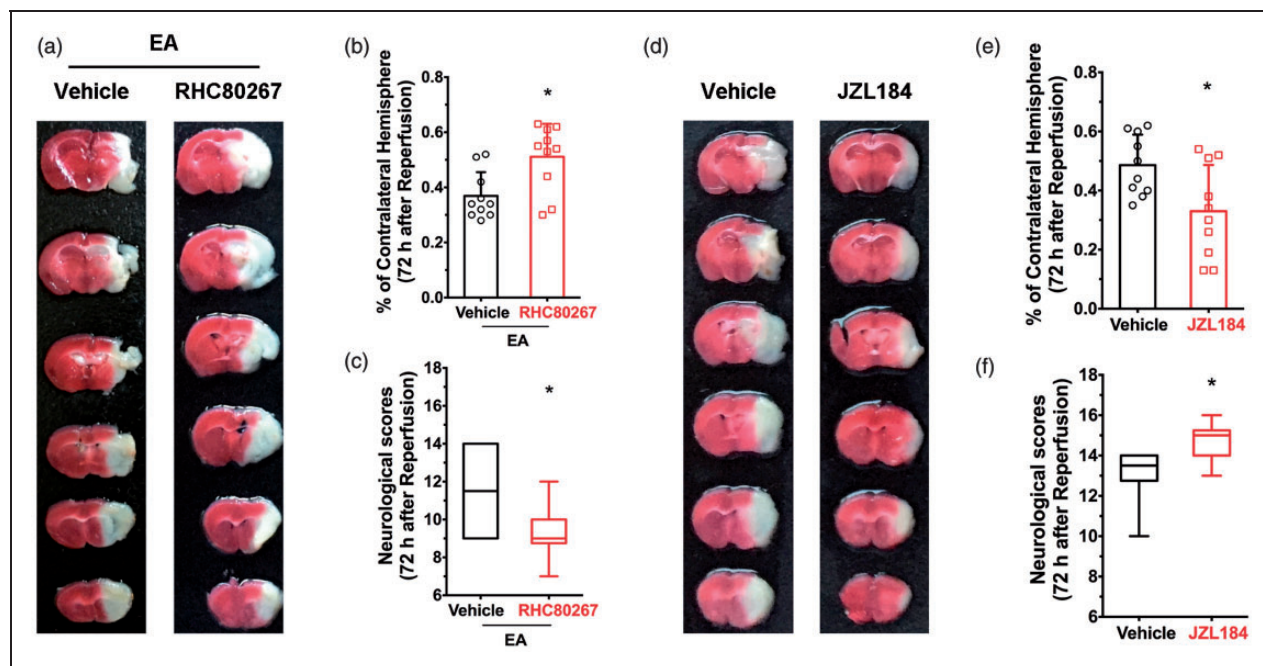


Figure 1. 2-AG mediates EA-induced neuroprotection. (a) Representative images showing infarct tissue following pretreatment with RHC80687 and vehicle. (b,c) EA-induced neuroprotection was abolished by pretreatment of RHC80687 with increased infarct volume (b) and lower neurological scores (c) compared with the vehicle group, induced by focal cerebral ischemia for 60 min. (d) Representative images showing infarct tissue following pretreatment with JZL184 and vehicle. (e,f) JZL184 pretreatment protected the ischemic penumbra from 60 min focal cerebral ischemia with smaller infarct volume (e) and higher neurological scores (f). Infarct volume graphs show mean \pm SD; $n = 10$ mice/group. * $p < 0.05$ vs. vehicle or wild-type littermates, t-test ((b): $p = 0.016$; (e): $p = 0.019$). Neurological behavioral scores show median (range) values; group differences tested using the Kruskal–Wallis test followed by the Mann–Whitney U test. * $p < 0.05$ vs. vehicle, U test ((c): $p = 0.0013$; (f): $p = 0.019$).

Ischemic penumbra astroglial CB_1R mediate the neuroprotective effects of EA pretreatment

To investigate the role of presynaptic CB_1R in producing neuroprotective effects of EA, two CB_1R antagonists (AM281 and NESS0327) were administered systemically 15 minutes before EA initiation. Both AM281 and NESS0327 groups had higher infarct volumes than the vehicle group (Figure 2(b) and (e)) and had lower the neurological scores (Figure 2(c) and (f)), suggesting that CB_1R mediate EA-induced neuroprotection. Cell specific CB_1R knockout mice were enrolled to determine which cell-specific CB_1R were involved in the neuroprotective effect of EA.

EA neuroprotection was lower in $GFAP-CB_1R-KO$ mice; infarct volume was higher in the knockout group compared to wild-type littermates following MCAO (Figure 2(h) and (i)), and neurological scores were lower (Figure 2(j)). In contrast, EA protection did not differentiate between GABAergic CB_1R and wild type, nor between glutamatergic CB_1R knockout mice and wild-type littermates (Figure 2(i) and (l)). These results suggest that activation of astroglial CB_1R is associated with EA-induced neuroprotection.

To clarify the effect of astroglial CB_1R in the ischemic penumbra, the AAV virus was injected into this brain region in CB_1R -floxed mice, which resulted in a deletion of astroglial CB_1R in the ischemic penumbral

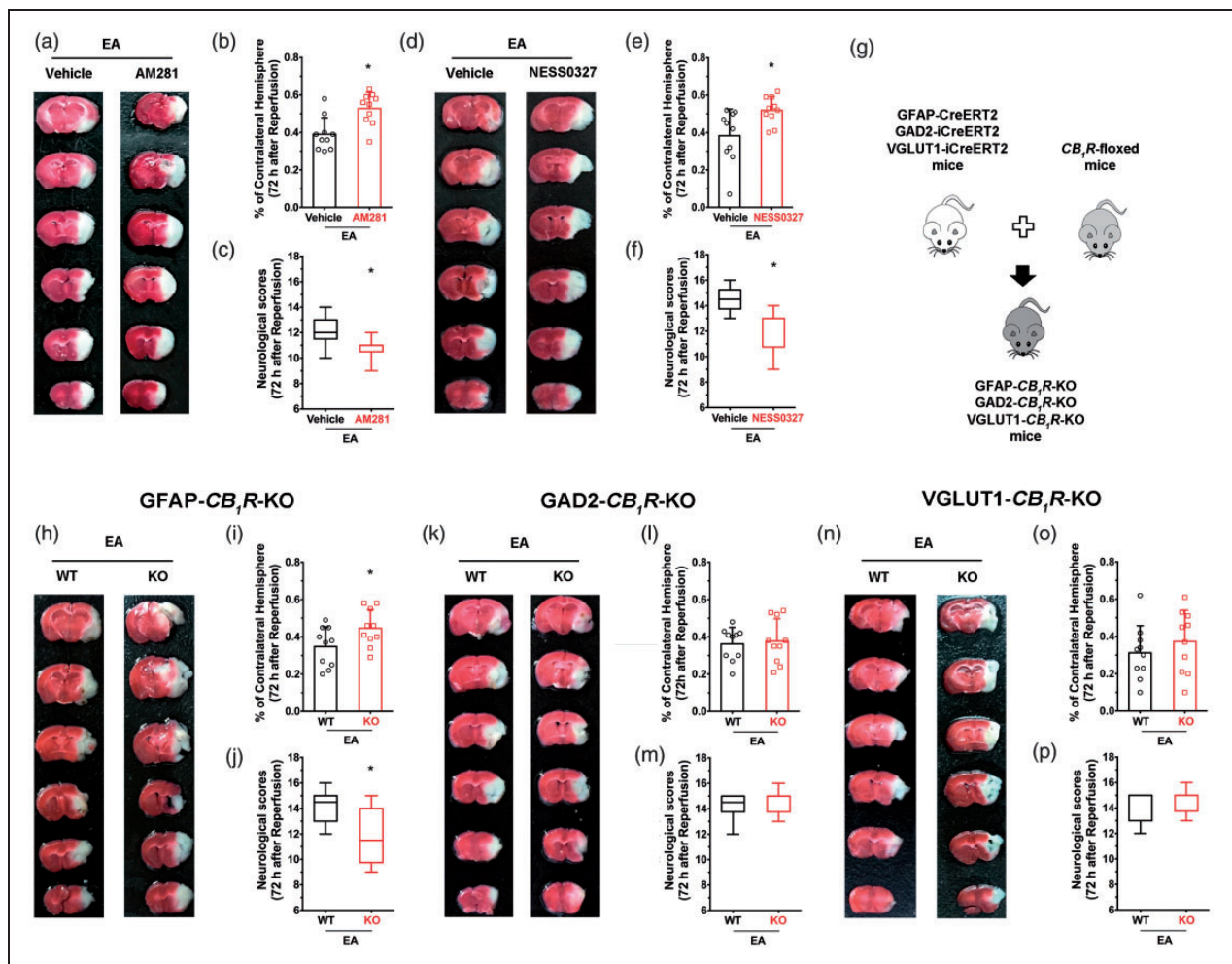


Figure 2. Ischemic penumbra astroglial CB_1R mediates the neuroprotective effects of EA pretreatment. (a) Representative images from AM281 and vehicle groups. (b–f) Blocking CB_1R with either AM281 or NESS0327 abolished the neuroprotective effect of EA pretreatment. (g) schematic showing generation of cell specific CB_1R deletion mice. (h) Representative images from $GFAP-CB_1R-KO$ and WT groups. (i,j) CB_1R deletion in astrocytes abolished the neuroprotective effect of EA pretreatment. (k–p) EA pretreatment did not produce neuroprotection both in $GAD2-CB_1R-KO$ mice and $VGLUT1-CB_1R-KO$ mice compared with their wild-type littermates. Infarct volume graphs show mean \pm SD, $n = 10$ mice/group. * $p < 0.05$ vs. wild-type littermates, t-test ((b): $p = 0.0023$; (e): $p = 0.0069$; (i): $p = 0.04$; (l): $p = 0.92$; (o): $p = 0.39$). Neurological behavioral score graphs show median (range) values; group differences were tested with the Kruskal–Wallis test followed by the Mann–Whitney U test. * $p < 0.05$ vs. vehicle, U test ((c): $p = 0.0093$; (f): $p = 0.01$; (j): $p = 0.016$; (m): $p = 0.58$; (p): $p = 0.68$).

(Figure 3(a) and (d)). This resulted in a higher infarct volume than the control virus group and lower neurological scores (Figure 3(e) to (g)), suggesting that ischemic penumbral astroglial CB_1R mediate EA-induced neuroprotection.

Activation of ischemic penumbra astrocytes mediate the neuroprotective effects of EA pretreatment

Activation of astroglial CB_1R mediate the neuroprotection of EA. The DREADD strategy was used to illuminate the function of ischemic penumbral astrocytes on the neuroprotective effect of EA pretreatment (Figure 4(a) and (b)). We assessed the severity of brain injury and found that there was no difference in

infarct volume (Figure 4(c) and (d)) or neurological scores (Figure 4(e)) between the hM3Dq group and the mCherry group. However, 72 hours after ischemic perfusion, infarct volume (Figure 4(c) and (d)) was higher and neurological scores (Figure 4(e)) were lower in the hM4Di group than in the mCherry group, suggesting that ischemic penumbral astrocytes are necessary for the EA-induced neuroprotection.

Ischemic penumbra astroglial CB_1R mediate the long-term neuroprotective effect of EA pretreatment

To determine whether the long-term neuroprotection of EA is via astroglial CB_1R , a CB_1R antagonist was tested in GFAP- CB_1R -KO mice. Systemic

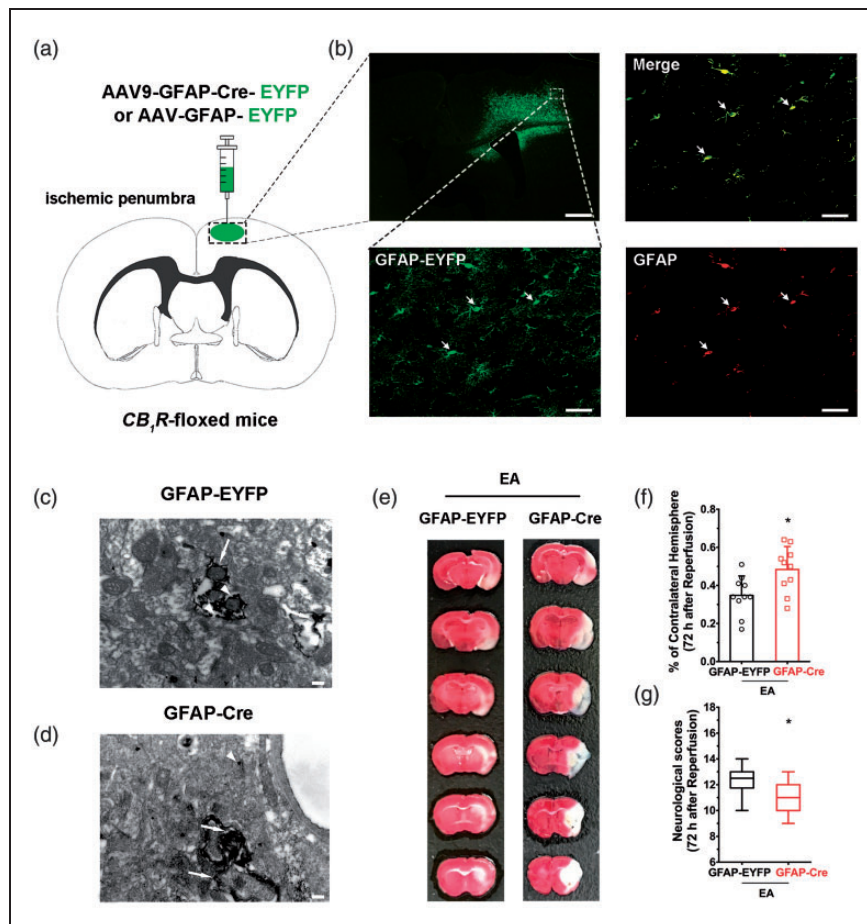


Figure 3. Ischemic penumbral astroglial CB_1R mediates the neuroprotective effects of EA pretreatment. (a) Schematic showing intra-ischemic penumbra injection of GFAP-Cre-EYFP or GFAP-EYFP virus in CB_1R -floxed mutant mice. (b) Coronal brain section showing the scope with green (GFAP-EYFP) fluorescence in the right ischemic penumbra after microinjection of different viruses. Corresponding magnified images ($40\times$) of the box in showing the virus (green), GFAP (red) and merge (yellow). Scale bar = $50\ \mu\text{m}$. (c, d) Electron microscopic images used to detect whether astroglial CB_1R is knocked out in the ischemic penumbra on CB_1R -floxed mice, showing a high density of CB_1R immune-positive silver grains (small arrows) in axons/terminals of GFAP-EYFP (c) but not in GFAP-Cre (d) mice. Scale bar = $200\ \text{nm}$. (e) Representative images showing infarct volume in GFAP-EYFP and GFAP-Cre mice. (f, g) Astroglial CB_1R deletion in ischemic penumbral abolishes the neuroprotective effect of EA pretreatment induced by focal cerebral ischemia for 60 min. Infarct volume graphs show mean \pm SD, $n = 10$ mice/group. $*p < 0.05$ vs. GFAP-EYFP group, t-test ((f): $p = 0.013$). Neurological behavioral score graphs show median (range) values; group differences were tested with the Kruskal–Wallis test followed by the Mann–Whitney U test. $*p < 0.05$ vs. GFAP-EYFP group, U test ((g): $p = 0.02$).

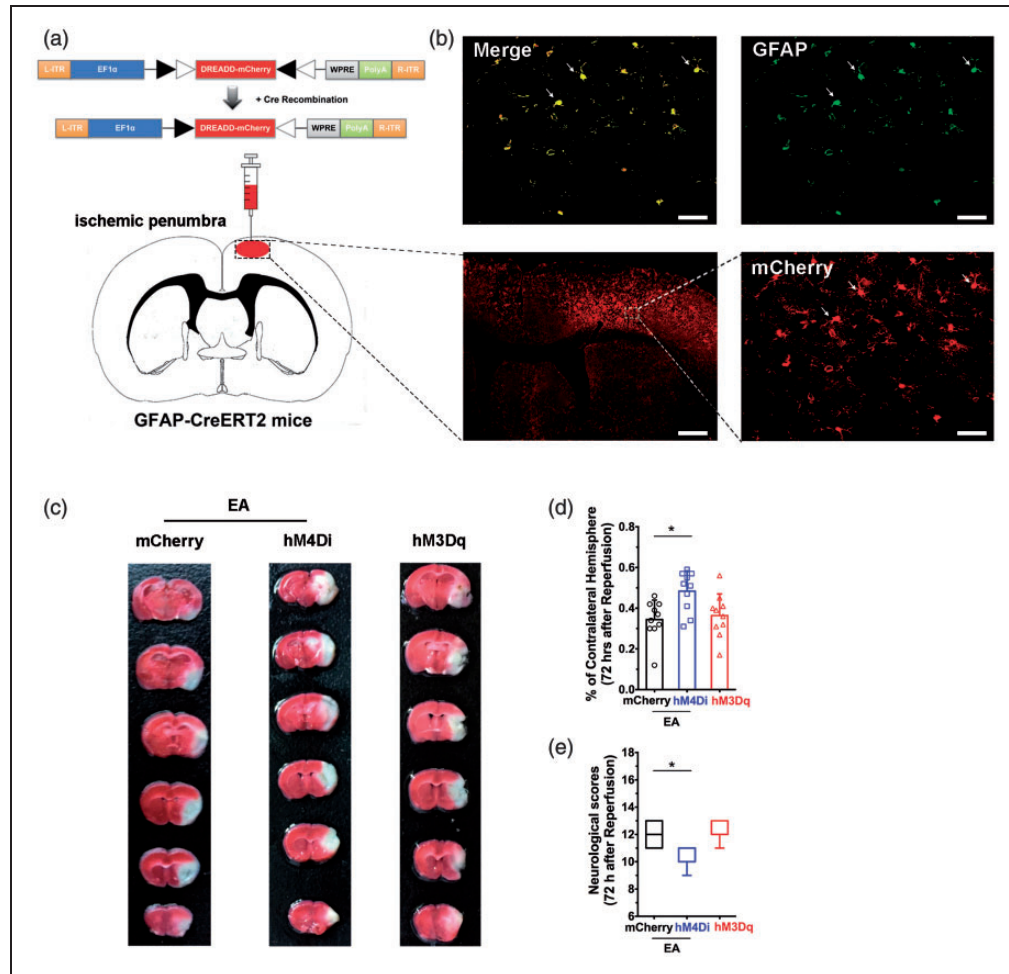


Figure 4. Ischemic penumbral astrocytes mediate the neuroprotective effects of EA pretreatment. (a) Schematic showing intra-ischemic penumbra injection of DREADD virus in GFAP-Cre mice. (b) Coronal brain section shows the scope with red (mCherry) fluorescence in the right ischemic penumbra after microinjection of different viruses. (c–e) corresponding magnified images (40 \times) of the box in (b) showing mCherry (red), GFAP, and merge (yellow). Scale bars = 50 μ m. (c) Representative images comparing infarct volume in mCherry, hM4Di, and hM3Dq groups. (d,e) Activation of ischemic penumbral astrocytes decreased infarct volume (d) and improved neurological scores (e) induced by focal cerebral ischemia for 60 min. By contrast, inhibition of ischemic penumbral astrocytes decreased infarct volume (d) and decreased neurological scores (e) after EA pretreatment. Infarct volume graphs show means \pm SD, $n = 10$ mice/group, * $p < 0.05$ vs. mCherry group, one-way ANOVA ((d): $p = 0.0023$; hM4Di vs mCherry; $p > 0.999$; hM3Dq vs. mCherry). Neurological behavioral score graphs show median (range) values; group differences were tested with the Kruskal–Wallis test followed by the Mann–Whitney U test. * $p < 0.05$ vs. mCherry group, U test ((e): $p = 0.0092$; hM4Di vs. mCherry; $p > 0.999$; hM3Dq vs. mCherry).

administration of the CB₁R antagonist AM281 led to higher infarct volume after MCAO than the vehicle group (Figure 5(a) and (d)) in addition to lower neurological test scores (Figure 5(e)). This result suggests that the EA-induced neuroprotection lasted for 28 days. Compared to wild-type littermates, infarct volume was higher in GFAP-CB₁R-KO mice after MCAO (Figure 5(f) to (i)), and neurological scores were lower (Figure 5(j)). This suggests that the astroglial CB₁R also mediate the long-term neuroprotection of EA pretreatment for 28 days. We then investigated the effect of early EA administration and found no

significant difference in infarct volume or neurological scores between the EA-pretreated group and sham EA group 28 days after MCAO (sFigure 3), suggesting no benefit from early EA pretreatment following an interval of this length.

EA pretreatment increases extracellular glutamate levels in the ischemic penumbra, which is neuroprotective

Astrocytes regulate the concentration of interstitial glutamate. To evaluate the impact of EA-induced

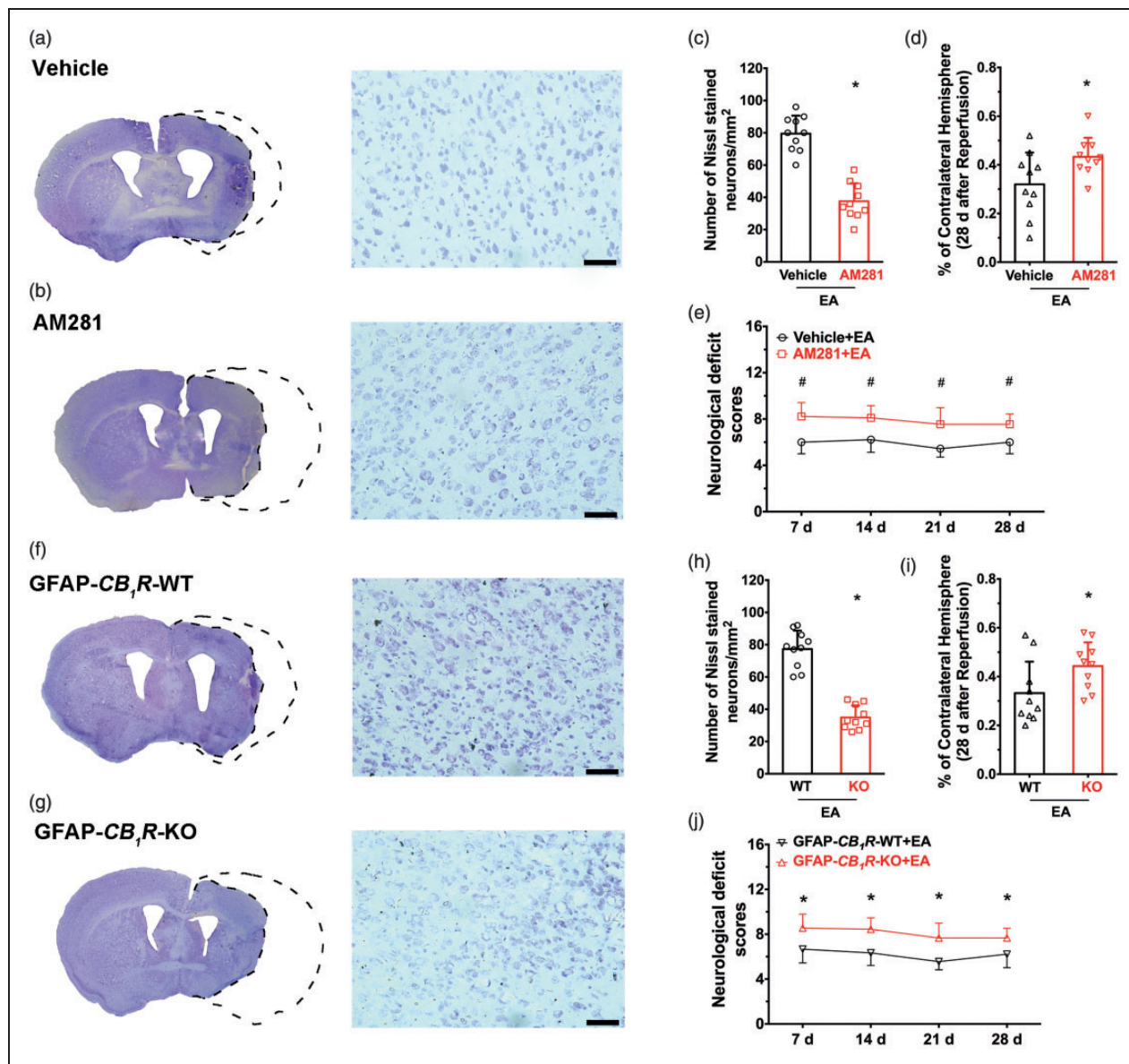


Figure 5. Ischemic penumbra astroglial CB₁R mediates the long-term neuroprotective effect of EA pretreatment. (a,b) Left images represent coronal sections of Nissl staining in (a) vehicle or (b) AM281 groups; Right images show higher magnifications (20×) of the images on the left. (c) Neuronal density ratio in the left/right cerebral cortex. EA-induced long-term neuroprotection is abolished by pretreatment with AM281 compared to the vehicle group, showing decreased infarct volume (d) and neurological deficit scores (e) induced by focal cerebral ischemia for 60 min. (f,g) Left images represent coronal sections of Nissl staining in the GFAP-CB₁R-WT (f) or GFAP-CB₁R-KO (g) groups; Right images show a higher magnification (20×) of the images on the left. (h) Neuronal density ratio in the left/right cerebral cortex. EA-induced long-term neuroprotection is abolished by pretreatment with GFAP-CB₁R-KO mice compared to wild-type littermates, showing decreased infarct volume (i) and neurological deficit scores (j) induced by focal cerebral ischemia for 60 min. Infarct volume graphs show mean \pm SD, $n = 10$ mice/group. * $p < 0.05$ vs. vehicle or wild-type littermates, t -test ((c): $p < 0.0001$; (d): $p = 0.03$ (h): $p < 0.0001$; (i): $p = 0.04$). Neurological deficit scores graphs show median (range) values; group differences were tested using the Kruskal–Wallis test followed by the Mann–Whitney U test. * $p < 0.05$ vs. wild-type littermates, U test ((e): $p = 0.004$; (j): $p = 0.005$).

activation of astrocytes on neurotransmitter release, *in vivo* microdialysis (Figure 6(a) and (b)) was employed. Extracellular fluid samples were detected and analyzed, and the concentration of extracellular glutamate in the ischemic penumbra was higher 0.5 hours and 2 hours

after EA pretreatment than the sham group (Figure 6 (c)), which suggests that EA-induced activation of astroglial CB₁R elevates glutamate levels.

Astroglial EAAT2 is the principal transporter that removes the excitatory neurotransmitter glutamate

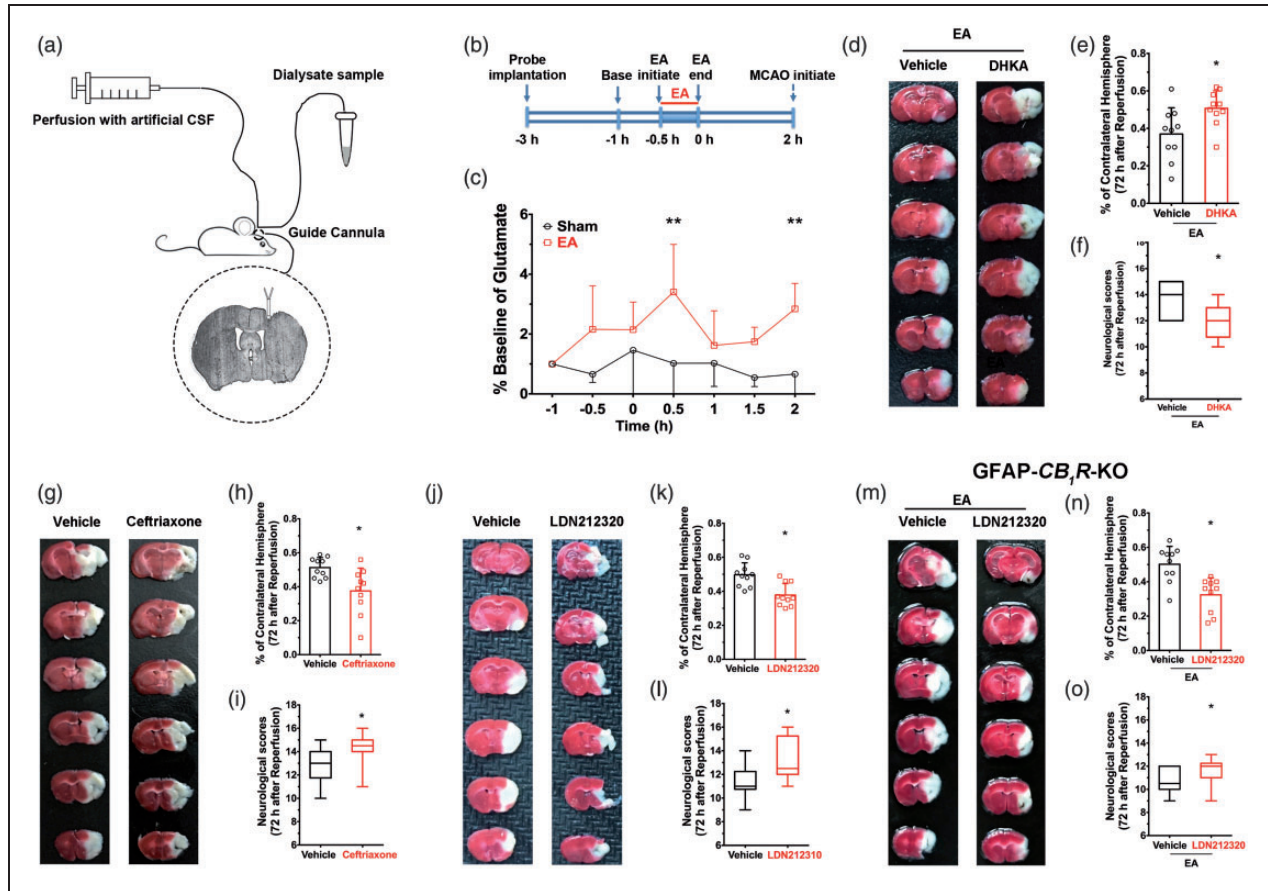


Figure 6. Pharmacological activation of EAAT2 restores EA-induced neuroprotective effect in astroglial CB_1R deficient mice by mediating the ambient glutamate. (a) Photomicrograph of the representative location of the tip of microdialysis probe in the ischemic penumbra. The vertical black arrow indicates the guide cannula and the lower black arrow represents the tip of microdialysis probe (microdialysis probe is 1 mm longer than guide cannula). (b) Timeline showing microdialysis experimental procedure. (c) EA pretreatment raised extracellular glutamate level in the ischemic penumbra 0.5 h and 2 h after administration of EA compared with the sham group ($*p_{0.5 h} = 0.025$ vs. sham, $*p_{2 h} < 0.007$ vs. sham, (c). (d–f) Pharmacological approaches were used to detect the role of EAAT2 in EA-induced neuroprotection. (d) Representative images comparing infarct volume in vehicle and DHKA (e,f) Inhibition of EAAT2 abolished the neuroprotective effect of EA pretreatment. (g,i) Representative images comparing infarct volume in vehicle and ceftriaxone (g) and in vehicle and LDN212320 (j). Activation of EAAT2 either by LDN212320 or Ceftriaxone decreased infarct volume (h,k) and improved neurological scores (i,l). (m–o) LDN212320 restored EA-induced neuroprotection in the GFAP- CB_1R -KO mice showing decreased infarct volume (n) and improved neurological scores (o) after MCAO compared with the vehicle group. Group differences in baseline dialysate glutamate concentrations were evaluated using one-way ANOVA with EA treatment as the between-subjects factor. Subsequently, per treatment dialysate glutamate levels were transformed to percentages of mean baseline dialysate concentration (set at 100%) for evaluation of changes in dialysate glutamate content following EA treatment as performed by ANOVA with repeated measures over time. In the case of significant overall effects, a Bonferroni multiple comparison test was used for post-hoc comparisons. Infarct volume graphs are shown as mean \pm SD, $n = 10$ mice/group. $*p < 0.05$ vs. vehicle, t-test ((e): $p = 0.001$; (h): $p = 0.0083$; (k): $p = 0.01$; (n): $p = 0.001$). Neurological behavioral scores graphs show median (range) values; group differences were tested using the Kruskal–Wallis test followed by the Mann–Whitney U test. $*p < 0.05$ vs. vehicle, U test ((f): $p = 0.019$; (i): $p = 0.02$; (l): $p = 0.01$; (o): $p = 0.04$).

from the extracellular space.²⁹ We used a neuropharmacological approach to detect the role of EAAT2 in EA-induced neuroprotection. When the EAAT2 inhibitor DHKA was injected systemically prior to EA, there was a higher infarct volume (Figure 6(e)) and lower neurological scores than the vehicle group (Figure 6(f)) 72 hours after EA administration and ischemic reperfusion. These results suggest that

inhibition of EAAT2 reversed the neuroprotective effect of EA. In contrast, systemic injection of either the EAAT2 translational activator, LDN212320, or the EAAT2 transcriptional activator, Ceftriaxone, led to lower infarct volume after MCAO (Figure 6(g), (h), (j) and (k)) and higher neurological scores (Figure 6(i) and (l)) than the vehicle group suggesting that the activation of EAAT2 mimicked the neuroprotective effect

of EA. These neuropharmacological results demonstrate that EAAT2 mediates the neuroprotective effect of EA.

Pharmacological activation of EAAT2 restores EA-induced neuroprotective effect in astroglial CB₁R-deficient mice

Both activation of astroglial CB₁R and EAAT2 mediate EA-induced neuroprotection. Nevertheless, the relationship between astroglial CB₁R and EAAT2 in EA-induced neuroprotection is unclear. To evaluate this issue, the EAAT2 activator LDN212320 was administered in GFAP-CB₁R-KO mice. After neurological scoring and TTC staining, an effect of administering LDN212320 was observed: seventy-two hour after reperfusion, infarct volume was higher (Figure 6 (m) and (n)) and neurological scores were lower (Figure 6(o)) in GFAP-CB₁R-KO mice than in the GFAP-CB₁R-WT group. These results suggest that activation of EAAT2 led to moderate upregulation of extracellular glutamate, which rescued EA neuroprotection in astroglial CB₁R knockout mice.

Discussion

In this study, we investigated the mechanism underlying the neuroprotective effect of EA pretreatment. First, we demonstrated that EA pretreatment elicited eCBs, which subsequently activated ischemic penumbra astroglial CB₁R, which led to cerebral ischemic protection. It has been shown that activation of astroglial CB₁R increases extracellular glutamate. Using microdialysis, we found that EA pretreatment increased interstitial glutamate in the ischemic penumbra by up-regulation of EAAT2. Our findings suggest that EA pretreatment induced an increase of ambient eCBs and subsequent activation of ischemic penumbra astroglial CB₁R led to the moderate upregulation of extracellular glutamate, which protected neurons from cerebral ischemic injury. These findings provide clear evidence for the cell-specific and brain region-specific mechanism underlying EA-induced neuroprotection.

Stroke is one of the leading causes of mortality and morbidity worldwide and results in cognitive, affective, and sensorimotor dysfunction.⁴ However, there are currently no efficacious interventions. Evoking endogenous protective mechanisms is a promising therapeutic approach for stroke patients. Our previous studies demonstrate that EA pretreatment develops a neuroprotective effect by reducing ischemic infarct volume, accompanied with higher neurological scores in rats.¹⁵ Subsequent studies^{16,18,46-50} show that several transmitters, modulators and molecular pathways, such as

certain neurochemicals (for example, opioid peptides and 5-hydroxytryptamine),^{47,51} cerebral blood flow,⁴⁶ apoptosis (cholecystokinin octapeptide (CCK-8)),^{47,48} inflammation⁴⁸⁻⁵⁰ and eCBs,^{16,18} regulate the ischemic tolerance effect of EA. Although Wang et al.¹⁸ and others demonstrated that eCBs are involved in the neuroprotective effect of EA,^{16,17} the detailed mechanism had not yet been described.

In recent years, neuroprotective effects of EA have been demonstrated in both animal studies and clinical trials. An accumulation of evidence indicates that EA can attenuate ischemic brain injury via specific mechanisms, such as regulating apoptosis or inflammation-related factors, which in turn regulate glutamate release, etc. Meanwhile, EA greatly enhances cerebral blood flow and promotes daily-life activity for stroke patients in clinics. Our results strongly indicate that the neuroprotective effect of EA pretreatment on cerebral ischemic injury occurs through the regulation of astroglial eCBs in the ischemic penumbra. This is a newly described neuroprotective mechanism that underlies EA and further confirms the value of the broad application of this approach in neurology.

Pharmacological intervention was used to up- and down-regulate the concentration of 2-AG before EA administration and it was found that when elevated, infarct volume increased, and when reduced, neurological outcomes following cerebral ischemia were better. Conversely, we noted that the neuroprotective effects of EA were reversed following inhibition of 2-AG. These results suggest that 2-AG mediates the neuroprotective effect of EA pretreatment. Two different CB₁R antagonists, AM281 and NESS0327, reversed the neuroprotective effect of EA. By employing mutant mice with knockout of CB₁R in either glutamergic neurons, GABAergic neurons or astrocytes, we found that the neuroprotective effect of EA was reversed by deletion of astroglial CB₁R, which indicated that astroglial CB₁R mediated the neuroprotective effect of EA. However, EA did not provide neuroprotection after ischemic stroke. As reported, monoacylglycerol lipase (MAGL) inhibitors such as JZL184 or MJN110, administered 60 minutes after stroke, produced neuroprotection against permanent focal cerebral ischemic injury.⁵² However, to apply this kind of intervention strategy as a better alternative to EA treatment in such a narrow therapeutic time window, further evidence is necessary to evaluate safety with regards to cerebral hemorrhage. Otherwise, widespread application of MAGL inhibitors remain limited by the narrow treatment time windows and the related risks of cerebral hemorrhage.

Several studies have demonstrated that interactions between astrocytes and surrounding cells can influence neuronal activity and brain injury outcomes.⁵³⁻⁵⁸

However, the function of astrocytes in EA-induced neuroprotection is unclear. Our previous finding demonstrated that long-term depression induced by endogenous cannabinoids produced neuroprotective effects via astroglial CB₁R after stroke in rodents,²⁹ which also indicates that astroglia are of great importance in neuroprotection. To determine whether astroglia participated in the EA-induced neuroprotective effects, we used a DREADD strategy. Excitation or inhibition of astrocytes in the ischemic penumbra by microinjection of the DREADD virus showed that excitation of astrocytes decreased infarct volume and improved neurological scores, while inhibition of astrocytes in the ischemic penumbra reversed the neuroprotective effect of EA, suggesting that activation of astrocytes protect neurons from ischemic injury.

When a sudden interruption of cerebral blood supply to a specific region of the brain happens within minutes, especially a reduction in the blood supply to under 15~20% of baseline levels, an irreversibly damaged infarct core with rapidly evolving necrotic cell death may occur. The ischemic penumbra offers a target for therapies in the treatment of stroke.^{59,60} By crossing *CB₁R*-floxed mice with GFAP-CreERT2 mutant mice to generate a GFAP-*CB₁R*-KO mouse line, we found that astroglial *CB₁R* is associated with EA-induced neuroprotection. Moreover, in order to eliminate side effects due to widespread astroglial *CB₁R* knockout in the whole brain, we specifically knocked out astroglial *CB₁R* in the primary motor cortex and found that deletion of ischemic penumbral astroglial *CB₁R* reversed the neuroprotective effect of EA.

We also found that the EA-induced neuroprotective effect lasted for 28 days. It has been demonstrated that endogenous protective mechanisms could be induced to the development of the neuroprotection by preconditioning.⁸⁻¹⁰ Therefore, we suppose that EA preconditioning also activates an endogenous protective mechanism, which then reduces brain damage produced during ischemia-reperfusion and contributes to brain function restoration, which subsequently leads to protracted protection (about 28 days). However, early EA pretreatment 28 days before MCAO showed no neuroprotective effect on ischemic stroke. The reason might be due to preconditioning windows of neuroprotection. It has been demonstrated that there are two specific time windows in which preconditioning can occur. The first window (rapid tolerance) appearing immediately after the preconditioning maneuver lasts no longer than 3 hours, and then the neuroprotective effect wears off, whereas a second window of neuroprotection (delayed tolerance) reappears 24 hours after preconditioning and lasts more than 12 hours.⁶¹⁻⁶⁴ Combined with the previous findings, an interval of

28 days may be too long to maintain the neuroprotective effect against ischemic stroke.

CB₁R are expressed at the membranes of neuronal presynaptic terminals responsible for the inhibition of neurotransmitter release.^{36,59} Postsynaptic depolarization leads to release of eCBs and then activation of presynaptic CB₁R and transient suppression of the release of inhibitory and excitatory neurotransmitters. The same eCB feedback mechanism operates at astroglial CB₁R and leads to the increase of extracellular glutamate. Recently, Wang et al.²⁹ demonstrated that acute elevation of extracellular eCB following eCB clearance inhibition results in neuroprotection through induction of long-term depression following sequential activation of astroglial CB₁R and postsynaptic glutamate receptors. We speculated that the EA produced mild long-term depression via activation of astroglial CB₁R, which increased glutamate. We employed *in vivo* microdialysis to detect the concentration of glutamate following EA administration in the ischemic penumbra. We found that the concentration of glutamate was increased in the ischemic penumbra after EA pretreatment, which suggests that EA-induced activation of astroglial CB₁R increased glutamate levels.

Glutamate clearance is necessary for proper synaptic activation and to prevent neuronal damage from excessive activation of glutamate receptors.⁶⁰ EAAT2 is the principal transporter that clears the excitatory neurotransmitter glutamate from the extracellular space at synapses in the central nervous system, and is responsible for over 90% of glutamate reuptake within the brain.^{65,66} The neuropharmacological results from the current study illustrate that activation of EAAT2 mimicked the neuroprotective effect of EA, whereas inhibition of EAAT2 reversed the neuroprotective effect of EA. Administration of the EAAT2 translational activator, LDN212320, in GFAP-*CB₁R*-KO mice rescued the neuroprotective effect of EA. This suggests that activation of EAAT2 leads to moderate upregulation of extracellular glutamate, which rescued EA neuroprotection in astroglial *CB₁R* knockout mice.

This study also has limitations. We used pharmacological methods to augment or reduce the concentration of 2-AG before administration of EA. The results showed that 2-AG mediated the neuroprotective effect of EA pretreatment. Nevertheless, we have not determined the cellular origin of EA-induced 2-AG. DAGL α and DAGL β both contribute substantially to the regulation of steady-state levels of 2-AG in the brain and other tissues.⁵⁹ Levels of 2-AG are reduced by up to 80% in the brain and spinal cord, and by ~90% in the liver in mice lacking DAGL α and DAGL β , respectively.⁶⁷ It follows that the concentration of 2-AG is dominated by DAGL α . Further study should employ cell-specific DAGL α knockout mice to

illuminate the origins of EA-induced 2-AG. In addition, we have not explained the mechanism by which activation of EAAT2 leads to moderate upregulation of extracellular glutamate in astroglial CB_1R knockout mice, which mediates the neuroprotective effect of EA. As we know, glutamate is an important excitatory neurotransmitter in the CNS. Under pathological conditions, such as ischemic stroke, the accumulation of extracellular glutamate stimulates NMDA receptors either on the neuron or the glial cells, leading to cell death through multiple pathways. EA pretreatment involves a variety of endogenous protective mechanisms. Further research should explore the underlying mechanism by which EAAT2 mediates glutamate-related neuroprotective effects of EA pretreatment.

In summary, the present study provides robust evidence for the cell-specific and brain region-specific mechanism of EA-induced neuroprotection. It is suggested that EA pretreatment induced an increase of ambient eCB and subsequent activation of ischemic penumbral astroglial CB_1R , which led to a moderate upregulation of extracellular glutamate to protect neurons from cerebral ischemic injury. These findings provide a more complete understanding of the neurobiological mechanism underlying the neuroprotective effects of EA pre-treatment and suggest a potential therapeutic target for ischemic stroke. EA pretreatment may also benefit the patients undergoing intracranial aneurysm procedure, which otherwise could result in cerebral ischemic injury.

Funding

The author(s) disclosed receipt of the following financial support for the research, authorship, and/or publication of this article: This study was supported by the International Cooperation and Exchange of the National Natural Science Foundation of China (No. 81420108013 to L.X.), National Natural Science Foundation of China (No. 81701362 to Y. C.), Guangdong Provincial Key Laboratory of Brain Connectome and Behavior (No. 2017B030301017), CAS Key Laboratory of Brain Connectome and Manipulation (No. 2019DP173024).

Acknowledgments

We thank Shiquan Wang for technical assistance. We thank David Bett for linguistic assistance during the preparation of this manuscript.

Declaration of conflicting interests

The author(s) declared no potential conflicts of interest with respect to the research, authorship, and/or publication of this article.

Authors' contributions

CY, JL, ZJ, JW, and AY conducted experiments and analyzed data, and contributed to writing the manuscript. XL, SY and XZ were involved in partial data analysis and manuscript writing. FW and LX designed the project and wrote the manuscript.

Supplementary material

Supplemental material for this article is available online.

ORCID iD

Feng Wang  <https://orcid.org/0000-0002-7547-3115>

References

1. Johnston SC, Mendis S and Mathers CD. Global variation in stroke burden and mortality: estimates from monitoring, surveillance, and modelling. *Lancet Neurol* 2009; 8: 345–354.
2. Hoyert DL and Xu J. Deaths: preliminary data for 2011. *Natl Vital Stat Rep* 2012; 61: 1–51.
3. Mozaffarian D, Benjamin EJ, Go AS, et al. Heart disease and stroke statistics-2016 update: a report from the American Heart Association. *Circulation* 2016; 133: e38–e360.
4. Chen G, Leak RK, Sun Q, et al. Neurobiology of stroke: research progress and perspectives. *Prog Neurobiol* 2018; 163-164: 1–4.
5. Powers WJ, Rabinstein AA, Ackerson T, et al. 2018 Guidelines for the early management of patients with acute ischemic stroke: a guideline for healthcare professionals from the American Heart Association/American Stroke Association. *Stroke* 2018; 49: e46–e110.
6. Ma H, Campbell BCV, Parsons MW, et al. Thrombolysis guided by perfusion imaging up to 9 hours after onset of stroke. *N Engl J Med* 2019; 380: 1795–1803.
7. Liebig T, Holtmannspotter M, Crossley R, et al. Metric-Based virtual reality simulation: a paradigm shift in training for mechanical thrombectomy in acute stroke. *Stroke* 2018; 49: e239–e242.
8. Nie H, Xiong L, Lao N, et al. Hyperbaric oxygen preconditioning induces tolerance against spinal cord ischemia by upregulation of antioxidant enzymes in rabbits. *J Cereb Blood Flow Metab* 2006; 26: 666–674.
9. Bordet R, Deplanque D, Maboudou P, et al. Increase in endogenous brain superoxide dismutase as a potential mechanism of lipopolysaccharide-induced brain ischemic tolerance. *J Cereb Blood Flow Metab* 2000; 20: 1190–1196.
10. Deplanque D, Gele P, Petrault O, et al. Peroxisome proliferator-activated receptor- α activation as a mechanism of preventive neuroprotection induced by chronic fenofibrate treatment. *J Neurosci* 2003; 23: 6264–6271.
11. Kato H, Kogure K, Araki T, et al. Immunohistochemical localization of superoxide dismutase in the hippocampus following ischemia in a gerbil model of ischemic tolerance. *J Cereb Blood Flow Metab* 1995; 15: 60–70.

12. Iadecola C and Anrather J. Stroke research at a crossroad: asking the brain for directions. *Nat Neurosci* 2011; 14: 1363–1368.
13. Mei ZG, Huang YG, Feng ZT, et al. Electroacupuncture ameliorates cerebral ischemia/reperfusion injury by suppressing autophagy via the SIRT1-FOXO1 signaling pathway. *Aging (Albany NY)* 2020; 12: 13187–13205.
14. Zhang BY, Wang GR, Ning WH, et al. Electroacupuncture pretreatment elicits tolerance to cerebral ischemia/reperfusion through inhibition of the GluN2B/m-Calpain/p38 MAPK proapoptotic pathway. *Neural Plast* 2020; 2020: 8840675.
15. Xiong L, Lu Z, Hou L, et al. Pretreatment with repeated electroacupuncture attenuates transient focal cerebral ischemic injury in rats. *Chin Med J (Engl)* 2003; 116: 108–111.
16. Du J, Wang Q, Hu B, et al. Involvement of ERK 1/2 activation in electroacupuncture pretreatment via cannabinoid CB1 receptor in rats. *Brain Res* 2010; 1360: 1–7.
17. Zhao JX, Tian YX, Xiao HL, et al. Effects of electroacupuncture on hippocampal and cortical apoptosis in a mouse model of cerebral ischemia-reperfusion injury. *J Tradit Chin Med* 2011; 31: 349–355.
18. Wang Q, Peng Y, Chen S, et al. Pretreatment with electroacupuncture induces rapid tolerance to focal cerebral ischemia through regulation of endocannabinoid system. *Stroke* 2009; 40: 2157–2164.
19. Breivogel CS and Childers SR. The functional neuroanatomy of brain cannabinoid receptors. *Neurobiol Dis* 1998; 5: 417–431.
20. Piomelli D. The molecular logic of endocannabinoid signalling. *Nat Rev Neurosci* 2003; 4: 873–884.
21. Stella N, Schweitzer P and Piomelli D. A second endogenous cannabinoid that modulates long-term potentiation. *Nature* 1997; 388: 773–778.
22. Herkenham M, Lynn AB, Johnson MR, et al. Characterization and localization of cannabinoid receptors in rat brain: a quantitative in vitro autoradiographic study. *J Neurosci* 1991; 11: 563–583.
23. Tsou K, Brown S, Sanudo-Pena MC, et al. Immunohistochemical distribution of cannabinoid CB1 receptors in the rat central nervous system. *Neuroscience* 1998; 83: 393–411.
24. Moldrich G and Wenger T. Localization of the CB1 cannabinoid receptor in the rat brain. An immunohistochemical study. *Peptides* 2000; 21: 1735–1742.
25. Massi P, Valenti M, Bolognini D, et al. Expression and function of the endocannabinoid system in glial cells. *Curr Pharm Des* 2008; 14: 2289–2298.
26. Liu Z, Han J, Jia L, et al. Synaptic neurotransmission depression in ventral tegmental dopamine neurons and cannabinoid-associated addictive learning. *PLoS One* 2010; 5: e15634.
27. Han J, Kesner P, Metna-Laurent M, et al. Acute cannabinoids impair working memory through astroglial CB1 receptor modulation of hippocampal LTD. *Cell* 2012; 148: 1039–1050.
28. Duan T, Gu N, Wang Y, et al. Fatty acid amide hydrolase inhibitors produce rapid anti-anxiety responses through amygdala long-term depression in male rodents. *J Psychiatry Neurosci* 2017; 42: 230–241.
29. Wang F, Han J, Higashimori H, et al. Long-term depression induced by endogenous cannabinoids produces neuroprotection via astroglial CB1R after stroke in rodents. *J Cereb Blood Flow Metab* 2019; 39: 1122–1137.
30. Globus MY, Busto R, Martinez E, et al. Comparative effect of transient global ischemia on extracellular levels of glutamate, glycine, and gamma-aminobutyric acid in vulnerable and nonvulnerable brain regions in the rat. *J Neurochem* 1991; 57: 470–478.
31. Chaudhry FA, Lehre KP, van Lookeren Campagne M, et al. Glutamate transporters in glial plasma membranes: highly differentiated localizations revealed by quantitative ultrastructural immunocytochemistry. *Neuron* 1995; 15: 711–720.
32. Rothstein JD, Dykes-Hoberg M, Pardo CA, et al. Knockout of glutamate transporters reveals a major role for astroglial transport in excitotoxicity and clearance of glutamate. *Neuron* 1996; 16: 675–686.
33. Rao VL, Dogan A, Bowen KK, et al. Antisense knockdown of the glial glutamate transporter GLT-1 exacerbates hippocampal neuronal damage following traumatic injury to rat brain. *Eur J Neurosci* 2001; 13: 119–128.
34. Weller ML, Stone IM, Goss A, et al. Selective overexpression of excitatory amino acid transporter 2 (EAAT2) in astrocytes enhances neuroprotection from moderate but not severe hypoxia-ischemia. *Neuroscience* 2008; 155: 1204–1211.
35. Chu K, Lee ST, Sinn DI, et al. Pharmacological induction of ischemic tolerance by glutamate transporter-1 (EAAT2) upregulation. *Stroke* 2007; 38: 177–182.
36. Kano M, Ohno-Shosaku T, Hashimoto-dani Y, et al. Endocannabinoid-mediated control of synaptic transmission. *Physiol Rev* 2009; 89: 309–380.
37. Percie Du Sert N, Hurst V, Ahluwalia A, et al. The ARRIVE guidelines 2.0: Updated guidelines for reporting animal research. *J Cereb Blood Flow Metab* 2020; 40: 1769–1777.
38. Zhong H, Tong L, Gu N, et al. Endocannabinoid signaling in hypothalamic circuits regulates arousal from general anesthesia in mice. *J Clin Invest* 2017; 127: 2295–2309.
39. Wang Y, Gu N, Duan T, et al. Monoacylglycerol lipase inhibitors produce pro- or antidepressant responses via hippocampal CA1 GABAergic synapses. *Mol Psychiatry* 2017; 22: 215–226.
40. Garcia JH, Wagner S, Liu KF, et al. Neurological deficit and extent of neuronal necrosis attributable to Middle cerebral artery occlusion in rats. Statistical validation. *Stroke* 1995; 26: 627–635.
41. Hata R, Mies G, Wiessner C, et al. A reproducible model of Middle cerebral artery occlusion in mice: hemodynamic, biochemical, and magnetic resonance imaging. *J Cereb Blood Flow Metab* 1998; 18: 367–375.
42. Deng J, Zhang J, Feng C, et al. Critical role of matrix metalloproteinase-9 in chronic high fat diet-induced cerebral vascular remodeling and increase of ischaemic brain injury in micedagger. *Cardiovasc Res* 2014; 103: 473–484.

43. Ma L, Wang L, Yang F, et al. Disease-modifying effects of RHC80267 and JZL184 in a pilocarpine mouse model of temporal lobe epilepsy. *CNS Neurosci Ther* 2014; 20: 905–915.
44. Wang Y and Zhang X. FAAH inhibition produces antidepressant-like effects of mice to acute stress via synaptic long-term depression. *Behav Brain Res* 2017; 324: 138–145.
45. Clark W, Gunion-Rinker L, Lessov N, et al. Citicoline treatment for experimental intracerebral hemorrhage in mice. *Stroke* 1998; 29: 2136–2140.
46. Vallon M, Chang J, Zhang H, et al. Developmental and pathological angiogenesis in the Central nervous system. *Cell Mol Life Sci* 2014; 71: 3489–3506.
47. Doyle KP, Simon RP and Stenzel-Poore MP. Mechanisms of ischemic brain damage. *Neuropharmacology* 2008; 55: 310–318.
48. Lan L, Tao J, Chen A, et al. Electroacupuncture exerts anti-inflammatory effects in cerebral ischemia-reperfusion injured rats via suppression of the TLR4/NF-kappaB pathway. *Int J Mol Med* 2013; 31: 75–80.
49. Shi Y, Zhang L, Pu H, et al. Rapid endothelial cytoskeletal reorganization enables early blood-brain barrier disruption and long-term ischaemic reperfusion brain injury. *Nat Commun* 2016; 7: 10523.
50. Cai W, Yang T, Liu H, et al. Peroxisome proliferator-activated receptor gamma (PPARgamma): a master gatekeeper in CNS injury and repair. *Prog Neurobiol* 2018; 163–164: 27–58.
51. Manni L, Albanesi M, Guaragna M, et al. Neurotrophins and acupuncture. *Auton Neurosci* 2010; 157: 9–17.
52. Choi SH, Arai AL, Mou Y, et al. Neuroprotective effects of MAGL (monoacylglycerol lipase) inhibitors in experimental ischemic stroke. *Stroke* 2018; 49: 718–726.
53. Zhao CC, Jiang MY, Zhang LY, et al. Peroxisome proliferator-activated receptor gamma participates in the acquisition of brain ischemic tolerance induced by ischemic preconditioning via glial glutamate transporter 1 in vivo and in vitro. *J Neurochem* 2019; 151: 608–625.
54. Ma Y, Jiang L, Wang L, et al. Endothelial progenitor cell transplantation alleviated ischemic brain injury via inhibiting C3/C3aR pathway in mice. *J Cereb Blood Flow Metab* 2020; 40: 2374–2386.
55. Lie ME, Gowing EK, Johansen NB, et al. GAT3 selective substrate l-isoserine upregulates GAT3 expression and increases functional recovery after a focal ischemic stroke in mice. *J Cereb Blood Flow Metab* 2019; 39: 74–88.
56. Zhao N, Xu X, Jiang Y, et al. Lipocalin-2 may produce damaging effect after cerebral ischemia by inducing astrocytes classical activation. *J Neuroinflammation* 2019; 16: 168.
57. Piao CS, Holloway AL, Hong-Routson S, et al. Depression following traumatic brain injury in mice is associated with down-regulation of hippocampal astrocyte glutamate transporters by thrombin. *J Cereb Blood Flow Metab* 2019; 39: 58–73.
58. Hayakawa K, Esposito E, Wang X, et al. Transfer of mitochondria from astrocytes to neurons after stroke. *Nature* 2016; 535: 551–555.
59. Di Marzo V. Endocannabinoids: synthesis and degradation. *Rev Physiol Biochem Pharmacol* 2008; 160: 1–24.
60. Meldrum BS. Glutamate as a neurotransmitter in the brain: review of physiology and pathology. *J Nutr* 2000; 130: 1007S–1015S.
61. Wang Q, Xiong L, Chen S, et al. Rapid tolerance to focal cerebral ischemia in rats is induced by preconditioning with electroacupuncture: window of protection and the role of adenosine. *Neurosci Lett* 2005; 381: 158–162.
62. Xiong L, Zheng Y, Wu M, et al. Preconditioning with isoflurane produces dose-dependent neuroprotection via activation of adenosine triphosphate-regulated potassium channels after focal cerebral ischemia in rats. *Anesth Analg* 2003; 96: 233–237, table of contents.
63. Zhang X, Xiong L, Hu W, et al. Preconditioning with prolonged oxygen exposure induces ischemic tolerance in the brain via oxygen free radical formation. *Can J Anaesth* 2004; 51: 258–263.
64. Pagliaro P, Gattullo D, Rastaldo R, et al. Ischemic preconditioning: from the first to the second window of protection. *Life Sci* 2001; 69: 1–15.
65. Danbolt NC. Glutamate uptake. *Prog Neurobiol* 2001; 65: 1–105.
66. Sato H, Tamba M, Ishii T, et al. Cloning and expression of a plasma membrane cystine/glutamate exchange transporter composed of two distinct proteins. *J Biol Chem* 1999; 274: 11455–11458.
67. Gao Y, Vasilyev DV, Goncalves MB, et al. Loss of retrograde endocannabinoid signaling and reduced adult neurogenesis in diacylglycerol lipase knock-out mice. *J Neurosci* 2010; 30: 2017–2024.